

This is the accepted manuscript made available via CHORUS. The article has been published as:

Single well or double well: First-principles study of 8H and 3C inclusions in the 4H SiC polytype

Mao-Sheng Miao and Walter R. L. Lambrecht

Phys. Rev. B **85**, 205318 — Published 29 May 2012

DOI: [10.1103/PhysRevB.85.205318](https://doi.org/10.1103/PhysRevB.85.205318)

Single well or double well: a first principles study of 8H and 3C inclusions in the 4H SiC polytype

Mao-Sheng Miao

Materials Research Lab., University of California Santa Barbara, CA, 93106 and
Beijing Computational Science Research Center, Beijing, 100089 P. R. China

Walter R. L. Lambrecht

Department of Physics, Case Western Reserve University, 10900 Euclid Ave. Cleveland, OH 44106-7079

Using first-principles calculations with a hybrid functional, we examined several fundamental issues for heterojunction structures formed by the same material but in different polytypes including the precise location of the boundary and the polarization. Particularly, we demonstrate that the inclusion of 8H in 4H SiC generates a single quantum well (QW) structure, rather than a double well consisting of two 3C region separated by a single hexagonal layer barrier. The level of the QW states for 8H and 3C inclusions are calculated to be 0.42 eV and 0.68 eV below the conduction band minimum of 4H SiC, in good agreement with the experiments.

PACS numbers: 73.21.Cd, 73.40.Lq, 61.72.Nn

I. INTRODUCTION

The most distinctive property of SiC is its ability to form many different polytypes,¹ among which the most frequently studied ones are 3C, 4H, and 6H. The structural variations are accompanied by a large variation in the electronic structures and properties, including the band gaps and the effective electron masses.^{2,3} Since the band gap can vary from 3.33 eV for 2H to 2.42 eV for 3C materials, growing different SiC polytypes in adjacent layers may form quantum wells (QW) or superlattices.⁴⁻⁶ The discovery of the frequent occurrence of 3C inclusions in 4H SiC caused by double stacking fault growth for heavily n-doped samples under annealing⁷⁻⁹ shows a possibility of fabricating QW structures¹⁰⁻¹² based on different SiC polytypes.

Recently the inclusion of the 8H polytype in 4H SiC was found in as-grown samples,^{13,14} which adds an interesting new member to the heteropolytype QWs. The major difference between the 8H inclusion and the 3C inclusion is the present of one extra hexagonal layer in the middle of the cubic layers. An important issue then arises: will the system behave like a single QW or like two adjacent wells separated by a single hexagonal layer? [Fig. 1] A recent work suggests the latter scenario by comparing the photoluminescence spectra and QW simulations based on the effective mass approximation.¹⁵ However, it is not entirely clear whether this approximation is valid for ultra-thin QW structure.

Another fundamental issue is general to all heterojunctions formed by polytypes: where is the boundary between different regions? For example in the 4H/3C/4H QW, the 4H region has alternating cubic and hexagonal layers, *hchchchc*..., whereas the 3C region only consists of cubic layers, *ccccc*.... Should the 3C region in a 4H/3C/4H QW starts from the first cubic layer and end at the last one? The situation is more complicated for the 4H/8H/4H QW. The sequence of cubic and hexago-

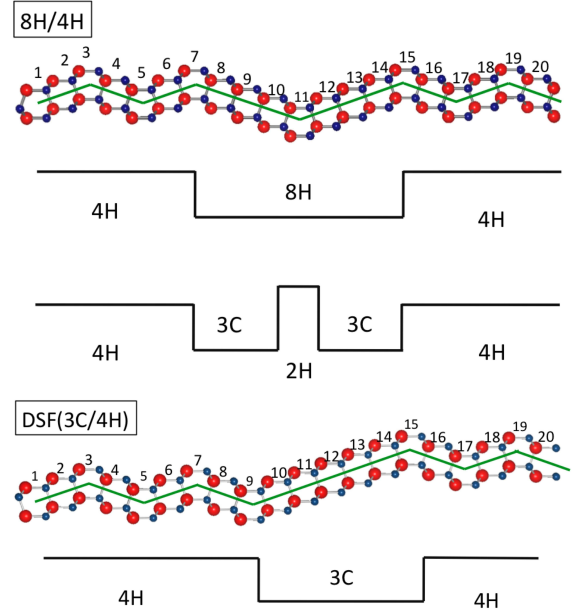


FIG. 1: Diagram of 8H and 3C inclusions in 4H SiC matrix. The single well and double well models of 8H inclusion in 4H SiC are shown. The large (red in color) and the small (blue) balls stand for the Si and the C atoms. The layers numbers denote the Si-C bilayers consisting of Si atoms in one stack and the C atoms occupying the preceding stack.

nal layers for 8H is *hccchccc*.... It is not *a-priori* clear which is the boundary layer between the 4H and 8H region. As a matter of fact, it is unclear whether there is a sharp boundary between the two polytypes. Another important feature of the SiC polytypes is the variation of the spontaneous polarization field. For bulk materials, the polarization is strong in 2H and 4H SiC, relatively weak in 8H and null in 3C SiC. It is interesting to examine how polarization changes when the polytypes form a

TABLE I: Structural parameters, total energies and band gaps calculated by HSE functions. For comparison, the experimental band gaps are also listed. The total energy is relative to the energy of 4H per atom.

	a (Å)	c/a	E_{tot} (meV)	E_g (eV)	E_g (exp.)
2H	3.0748	1.634	3.3	3.219	3.30 ²²
4H	3.0711	1.637	0.0	3.211	3.265 ²³
6H	3.0715	1.636	0.1	2.980	3.023 ²⁴
8H	3.0728	1.635	0.2	2.722	2.80 ²
3C	3.0741	1.633	0.7	2.263	2.39 ²

QW or superlattice structure.

II. METHOD AND QW MODEL

In order to study the QW state of heteropolytype QW and address the issue of polarization, polytype boundary and whether the 8H inclusion is a single well or a double well, we perform first principles calculations for an 4H/8H/4H and a 4H/3C/4H QW model structures. The calculations are performed by means of the Vienna Ab-initio Simulation Package (VASP) program.^{16,17} The Projector Augmented Wave (PAW) potentials^{18,19} and the Heyd-Scuseria-Ernzerhof (HSE) hybrid functional^{20,21} with 25% mixing of Hartree-Fock exchange are used in the calculations. The calculated band gaps for the bulk materials are in very good comparison with the experimental values. For example, as shown in Table I, the low temperature band gaps of 3C, 4H and 8H are 2.39 eV, 3.27 eV and 2.80 eV respectively, whereas they are obtained by HSE as 2.26 eV, 3.21 eV and 2.72 eV. HSE also resolves nicely the total energies of different polytypes. It agrees well with the experiments and the previous calculations on the order of polytype stability,^{25–27} *i.e.* 4H is most stable and 2H is significantly higher than 3C and 4H. The total energies of 6H and 8H are in between those of 3C and 4H.

Our QW calculations are performed for a supercell containing 20 bi-layers of Si and C. For 4H/8H/4H QW [Fig. 1], the sequence of the stacking²⁸ is ABCBAB—CBACBCAB—CBABCB or $\uparrow\uparrow\downarrow\downarrow\uparrow\uparrow \mid \downarrow\downarrow\downarrow\uparrow\uparrow\uparrow \mid \downarrow\downarrow\uparrow\uparrow\downarrow\downarrow$, or *hchchchccchccchchc*, where parallel spins mean cubic *c* and antiparallel spins means hexagonal *h* stacking. The size of the nominal 8H region is 8 bi-layers which is about 2 nm wide. Similarly, the sequence for 4H/3C/4H QW is ABCBABC—ABCABC—ACBCAC or $\uparrow\uparrow\downarrow\downarrow\uparrow\uparrow\downarrow \mid \uparrow\uparrow\uparrow\uparrow\uparrow \mid \downarrow\downarrow\uparrow\uparrow\downarrow\downarrow$, or *hchchchchccccchchc*. The calculation results including the layer-by-layer partial density of states (PDOS) and the wavefunctions of the QW states are shown in Fig. 2 for 8H inclusions and in Fig. 4 for 3C inclusions.

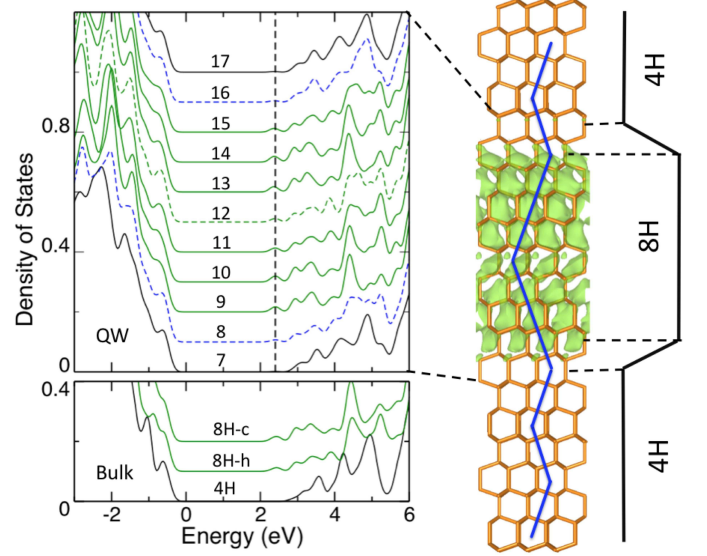


FIG. 2: The layer-by-layer PDOS and the wavefunction (shown as green isosurface in the right panel) of the QW state of an 8H inclusion in 4H. The layer number is as shown in Fig. 1. For comparison, the PDOS of cubic and hexagonal layers of 8H and the DOS of bulk 4H are also shown.

III. RESULTS

By comparing the layer PDOS of 8H/4H QW with the PDOS of bulk 4H and 8H SiC, we can identify the regions of 4H and 8H in the QW. As shown in Fig. 2, the PDOS of layers 9 to 15 can be identified as 8H layers, whereas layers 1-7 and 17-20 are 4H layers. The major difference is the existence of states at the energy of about 2.4 eV. Interestingly, not only the cubic layers but also the hexagonal layer in the 8H region show this QW state. Indeed the PDOS of layers 9 to 15 show similar PDOS, indicating that the QW states are uniformly distributed in 8H, a feature of single QW structure. The wavefunction of the QW state as shown in Fig. 1 also indicates that the 4H/8H/4H behaves as a single QW. On the other hand, we do notice a reduction of the wavefunction amplitude and the PDOS value at the center of the 8H region (layer 12), indicating a strong barrier effect of the 2H layer at the center of 8H region. This layer's PDOS is different from the hexagonal layers in bulk 8H, the PDOS of which, as shown in Fig. 2, is almost identical to the PDOS of a cubic layer, indicating the uniform distribution of the band edge wavefunctions throughout a given polytype. The layers 8 and 16 show a PDOS that is almost identical to 4H. Therefore, the 8H region can be considered to be only 7 layers instead of 8 layers thick and it has a quite clear boundary to 4H regions.

Our calculations confirm that the 4H/8H/4H is of type II, *i.e.* the electron QW states are localized in the 8H region whereas the hole QW states localize in the 4H region. The energy difference between the electron and the hole state is found to be 2.74 eV. This value is very close

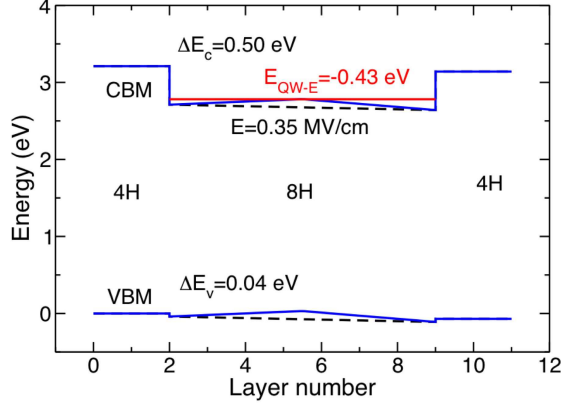


FIG. 3: The band diagram of 4H/8H/4H QW. The energies are aligned to the VBM position of bulk 4H SiC. The red line shows the first electronic state in the QW. The black lines show the average spontaneous potential in the QW. The electric field inside the QW is calculated to be around 0.35 MV/cm.

to the low temperature PL measurements of 2.72 eV^{14,29} and 2.672 eV¹⁵. In a recent study, Robert *et al.*¹⁵ found that the recombination energy is overestimated by about 200 meV by an effective mass approach for a single QW model. They argue that a double well model that consists of two 3C wells separated by a single 2H barrier layer can reduce the recombination energy to 2.68 which is in good comparison with the experimental PL value. They thus concluded that 8H inclusion in 4H should actually be treated as a double quantum well. Our calculations do not agree with this conclusion. We think the overestimate of the recombination energy is caused by the use of the effective mass approximation, which is not applicable to this ultra-thin quantum well system.

Next, we check the position of the QW level, which is the CBM of our model system, relative to the CBM of ideal 4H SiC. In order to compare the absolute value of these two systems, we line up the electrostatic potential at PAW sphere of the C atom in the center of the 4H region in our model system and the same potential of the C atom in bulk 4H. A sketch of the band diagram and the first electronic state in 4H/8H/4H QW is shown in Fig. 3. It is interesting to notice that this value is larger than that of a single stacking fault (0.27 eV)^{25,31} and smaller than that of a double stacking fault (0.67 eV).^{32,33} We found that the QW state in the 8H region is 0.43 eV below the CBM of bulk 4H, which is in good agreement with the experimental value of 0.39 eV.^{12,30} This might be attributed to the smaller valence band offset (VBO) for 8H/4H. The VBO and the conduction band offset (CBO) are obtained to be 0.04 eV and 0.50 eV respectively. The CBO is about 0.2 eV smaller than those of 3C in 4H³⁴ and 3C in 2H.⁵ The differences in VBO are much less significant.

The 4H/3C/4H QW has been studied in a similar fashion, and the results are shown in Fig. 4. The region of

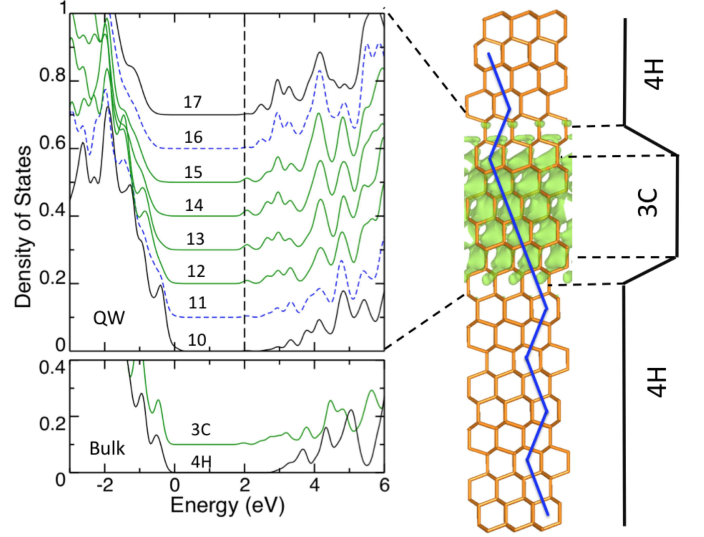


FIG. 4: The layer-by-layer PDOS and the wavefunction of QW state of 3C inclusion in 4H. The layer number is as shown in Fig. 1. For comparison, the DOS of bulk 3C and 4H are also shown.

PDOS that shows obvious 3C features (a peak at around 2.1 eV from the VBM) ranges from layer 12 to layer 15, which covers 4 layers in contrast to the 5 cubic layers in the DSF model. The boundary layers (11 and 16) show very small feature of 3C around 2.1 eV, indicating that the QW state penetrates into these layers. In addition, the location of the QW state also shows a distinct shift toward the right hand side of the QW because the cubic layers in the DSF model starts from layer 10 and extend to layer 14. The extension and the shift of the QW state can also be seen from the wavefunction of the QW state which is also shown in Fig. 4. As will be discussed below, the shift of the QW state is the result of strong polarization field in the 4H/3C/4H QW.

The QW state is found to be at 0.68 eV below the CBM of 4H SiC. This value is very close to the value of 0.67 eV obtained by local density functional (LDA)^{32,33} indicating that the position of the QW state can be well captured by local and semi-local functionals. The VBO and the CBO are found to be 1.01 eV and 0.014 eV. The 4H/3C/4H is also a type-II quantum well with very shallow barrier for the holes.

At last, we study the polarization of heterojunctions formed by SiC polytypes. We plot the electrostatic potentials at the PAW spheres of all the C atoms [Fig. 5 (a) and (b)]. The potential profiles obtained from the plane-averaged electrostatic potential show same features and values as Fig. 5. As shown in Fig. 5, the polarization potential varies more significantly in 4H/3C/4H QW than in 4H/8H/4H QW. The large polarization field in 4H/3C/4H QW may cause a large shift of the QW state. This effect can also be seen in a one-dimensional Schrödinger-Poisson simulation. In this simulation, the size of the QW is chosen the same as the width of the

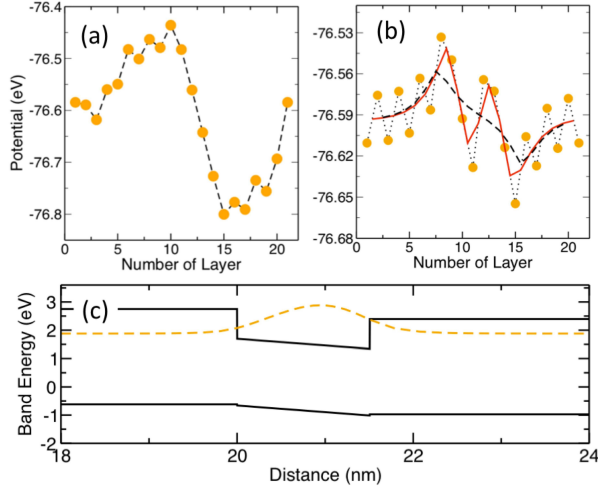


FIG. 5: (a) The average electrostatic potential of a SiC heteropolytype QW formed by a 3C inclusion in 4H. (b) The average electrostatic potentials of an 8H inclusion in 4H, in which the dotted, the solid and the dashed lines are averaged over 2, 4 and 8 layers respectively; please note the different scale. (c) Band diagram of a 3C inclusion in 4H SiC with simulated 1D wavefunction.

DSF. The parameters such as the CBO and VBO are chosen from the values obtained earlier in this paper. As shown in Fig. 5(c), the center of the wavefunction has been shifted from the center of the QW toward the right by the polarization field. More importantly, the amplitude of the wavefunction at the right edge of the QW is significantly larger than that at the left side, and the wavefunction penetrates deeply ($3 - 5 \text{ \AA}$ or $1 - 2$ layers) into the 4H region. This explains the observed shift of the 3C features in the calculated PDOS.

The problem whether a 4H/8H/4H QW should be considered a single or double well can also be viewed from the point of view of the polarization potential. For a single well, we expect a monotonic function, for a double well, we expect a W-shaped potential. The potential shows a zig-zag shape in the 4H region and a W shape in the 8H region [see Fig. 5(b)]. After make a running average of every 4-layers (solid line), the potential in 4H region become smooth and monotonic, whereas in the 8H region it retains a W shape. However, if we increase the number of layers over which we average to eight, the potentials in both 4H and 8H regions are smooth and monotonic. This slope should corresponds to the difference in polarization of 8H and 4H. We also note that the W-shaped barrier in potential in the 8H region is much smaller than the VBO and does not warrant considering the system as a double well, but rather as a single well with a little bump in the middle.

IV. CONCLUSIONS

In this paper, we studied some fundamental issues for heterojunctions formed by SiC polytypes: namely the question of how to locate the boundary between the layers, the nature of the QW localized states, and the polarization induced potentials by applying first-principles calculations. The importance of understanding these issues goes beyond SiC. Although the energy differences between different polytypes for other materials than SiC are usually much larger in comparison with those for SiC, these energy differences vary with the size of the crystallite and therefore the polytypes and the corresponding heteropolytype structures may form at the nano-scale.³⁵⁻³⁷

Our calculations show that the 8H inclusion in 4H matrix should be treated as a single quantum well rather than a double QW consisting of two thin regions of 3C and a hexagonal barrier layer at the center. Although both 8H and 3C inclusions show a distinctive boundary to the 4H regions, it may differ to the nominal boundary in the constructed model. The lowest QW state in a 4H/3C/4H QW shifts toward the right and penetrates into the 4H region due to the strong polarization field. Our calculations also yield the positions of QW states, the conducting and valence band offsets in good comparison with available experimental results. Furthermore, we found that polarization is a local property and the total potential shift over a region of non-zero polarization can be obtained by adding the contributions of single layers.

Acknowledgment The work is partially supported by ONR. M.-S. M. thanks the ConvEne-IGERT Program (NSF-DGE 0801627). The calculations were performed at the Ohio Supercomputing Center (OSC) under project PDS0145 and at the high performance computing clusters run by the California NanoSystems Institute (CNSI).

- ¹ *Properties of Advanced Semiconductor Materials: GaN, AlN, InN, BN, SiC, SiGe*, ed. by M. E. Levinshtein, S. L. Rumyantsev, and M. S. Shur, John Wiley & Sons, Inc. (2001).
- ² W. J. Choyke, D. R. Hamilton and L. Patrick, Phys. Rev. **133**, 1163 (1964).
- ³ W. R. L. Lambrecht, S. Limpijumnong, S. N. Rashkeev, and B. Segall, Phys. Stat. Solidi (b) **202**, 5-33, (1997).
- ⁴ F. Bechstedt and P. Käckell, Phys. Rev. Lett. **75**, 2180 (1995).
- ⁵ M. S. Miao and W. R. L. Lambrecht, Phys. Rev. B **68**, 155320 (2003).
- ⁶ San-huang Ke, Jian Zi, Kai-ming Zhang, and Xi-de Xie, Phys. Rev. B **54**, 8789 (1996).
- ⁷ R. S. Okojie, M. Xhang, P. Pirouz, S. Tumakha, G. Jessen, and L. Brillson, Appl. Phys. Lett. **79**, 3056 (2001).
- ⁸ L. J. Brillson, S. Tumakha, G. H. Jessen, R. S. Okojie, M. Zhang, P. Pirouz, Appl. Phys. Lett. **81**, 2785 (2002).
- ⁹ J. Q. Liu, H. J. Chung, T. Kuhr, Q. Li, and M. Skowronski, Appl. Phys. Lett. **80**, 2111 (2002).
- ¹⁰ S. Bai, R. P. Devaty, W. J. Choyke, U. Kaiser, G. Wagner, and M. F. MacMillan, Appl. Phys. Lett. **83**, 3171 (2003).
- ¹¹ Y. Ding, K. -B Park, J. P. Pelz, K. C. Palle, M. K. Mikhov, B. J. Skromme, H. Meidia and S. Mahajan, Phys. Rev. **69**
- ¹² K. -B Park, Y. Ding, J. P. Pelz, M. K. Mikhov, Y. Wang, and B. J. Skromme, Appl. Phys. Lett. **86**, 222109 (2005).
- ¹³ H. Fujiwara, T. Kimoto, T. Tojo and H. Matsunami, Mater. Sci. Forum, **483-485**, 151 (2005).
- ¹⁴ S. Izumi, H. Tsuchida, T. Tawara, I. Kamata and K. Izumi, Mater. Sci. Forum, **483-485**, 323 (2005).
- ¹⁵ T. Robert, S. Juillaguet, M. Marinova, T. Chassagne, I. Tsiaoussis, N. Frangis, E. K. Polychroniadis and J. Camassel, Mater. Sci. Forum, **615-617**, 339 (2009).
- ¹⁶ G. Kresse and J. Hafner, Phys. Rev. B **47**, 558 (1993);
- ¹⁷ G. Kresse and J. Furthmuller, Phys. Rev. B **54**, 11169 (1996).
- ¹⁸ P. E. Blochl, Phys. Rev. B **50**, 17953 (1994).
- ¹⁹ G. Kresse and D. Joubert, Phys. Rev. B **59**, 1758 (1999).
- ²⁰ J. Heyd, G. E. Scuseria, and M. Ernzerhof, J. Chem. Phys. **118**, 8207 (2003).
- ²¹ J. Heyd, G. E. Scuseria, and M. Ernzerhof, J. Chem. Phys. **124**, 219906 (2006).
- ²² L. Patrick, D. R. Hamilton, and W. J. Choyke, Phys. Rev. **143**, 526 (1966)
- ²³ L. Patrick, W. J. Choyke, and D. R. Hamilton, Phys. Rev. **137**, A1515 (1965)
- ²⁴ W. J. Choyke and Lyle Patrick, Phys. Rev. **127**, 1868 (1962)
- ²⁵ M. S. Miao, S. Limpijumnong and W. R. L. Lambrecht, Appl. Phys. Lett. **79**, 4360 (2001).
- ²⁶ S. Limpijumnong and W. R. L. Lambrecht, Phys. Rev. B **57**, 12017 (1998).
- ²⁷ V. Heine, C. Cheng and R. J. Needs, J. Am. Ceram. Soc. **74**, 2630 (1991).
- ²⁸ For a full description of the stacking notations, see *e.g.* Ref. 5 Briefly, the Si and C atoms each form close packed layers, *A, B, C* refer to the different sites the next layer can be deposited on a closed packed layer of spheres, \uparrow, \downarrow mean we go up in the alphabet in the *ABC* notation, and *c* (*h*) mean parallel (antiparallel) "pseudospins" $\uparrow\uparrow$ ($\uparrow\downarrow$).
- ²⁹ G. Feng, J. Suda and T. Kimoto, Appl. Phys. Lett. **92**, 221906 (2008).
- ³⁰ K. Park, *Electronic properties of stacking-fault induced heterostructures in silicon carbide studied with ballistic electron emission microscopy*, Ph. D thesis, Ohio State University (2006).
- ³¹ H. Iwata, U. Lindefelt, S. Öberg and P. R. Briddon, Phys. Rev. B **65**, 033203 (2001); H. Iwata, U. Lindefelt, S. Öberg, and P. R. Briddon, Mater. Sci. Forum, **389-393**, 529 (2002); J. Phys. Condens Matter **14**, 12733(2002).
- ³² U. Lindefelt, H. Iwata, S. Öberg, and P. R. Briddon, Phys. Rev. B **67**, 155204 (2003).
- ³³ W. R. L. Lambrecht and M. S. Miao, Phys. Rev. B **73**, 155312(2006).
- ³⁴ M. S. Miao and W. R. L. Lambrecht, J. Appl. Phys. **101**, 103711 (2007).
- ³⁵ D. Spirkoska, *et al.*, Phys. Rev. B **80**, 245325 (2009).
- ³⁶ I. Zardo, S. Conesa-Boj, F. Peiro, J. R. Morante, J. Arbiol, E. Uccelli, G. Abstreiter, and A. Fontcuberta i Morral, Phys. Rev. B **80**, 245324 (2009).
- ³⁷ P. Mélinon, *et al.* Nat. Mat. **6**, 479 (2007).